Widely Tunable Terahertz-Generating Semiconductor Disk Laser

Ksenia A. Fedorova,* Heyang Guoyu, Matthias Wichmann, Christian Kriso, Fan Zhang, Wolfgang Stolz, Maik Scheller, Martin Koch, and Arash Rahimi-Iman*

The demand for tunable terahertz (THz) generating laser sources is significantly growing as they are used in a wide range of applications including THz imaging, spectroscopy, and metrology. However, the development of THz systems for the use in many practical applications is generally impeded by the limited availability of compact, sufficiently powerful and cost-effective room-temperature sources in the desired spectral ranges. Herein, the development of a compact, continuous-wave, room-temperature, tunable THz-generating laser source in the 0.79–1.11 THz spectral region is reported. The laser source is based on intracavity difference-frequency generation in an aperiodically poled lithium niobate (aPPLN) crystal within a dual-wavelength vertical-external-cavity surface-emitting laser. Furthermore, spectral coverage in the THz domain is compared for such a device utilizing a periodically poled lithium niobate (PPLN) and an aPPLN crystal. The demonstrated results pave the way to an effective approach for the development of high-performance, room-temperature, widely tunable THz lasers for a variety of applications in science and industry.

Terahertz (THz) technology has been developing at a rapid pace throughout the past two decades due to a plethora of applications, which are presently evolving ranging from industrial inspection[1–3] to security applications.[4,5] In this respect, tunable powerful THz laser sources operating in the 0.8–2 THz range have attracted enormous attention over the past decades. In combination with THz cameras,[6] they hold a great potential for THz imaging[7] and holography.[8]

Several approaches have been taken to develop narrow-linewidth tunable room-temperature THz sources. These include photomixers,[9–12] parametric sources,[13–15] and quantum cascade lasers (QCLs).[16] However, most of these systems inherit

Dr. K. A. Fedorova, Dr. H. Guoyu, Dr. M. Wichmann, C. Kriso,
Dr. F. Zhang, Prof. W. Stolz, Dr. M. Scheller, Prof. M. Koch,
Dr. A. Rahimi-Iman
Department of Physics and Materials Sciences Center
Philipps-Universität Marburg
Marburg 35032, Germany
E-mail: ksenia.fedorova@physik.uni-marburg.de;
a.r-i@physik.uni-marburg.de

The ORCID identification number(s) for the author(s) of this article can be found under https://doi.org/10.1002/pssr.202000204.

a number of limitations, ranging from high cost and bulkiness to limited tunability and low power efficiency. Recently, THz frequency combs based on difference-frequency generation (DFG) from a mid-infrared QCL[17,18] have provided another effective approach to generating THz at room temperature, although the THz output is still in the range of a few microwatts. Recently, also intrinsic Josephson junction devices were reported to emit sub-mW power levels of THz and showed broad THz tunability, however, their operation is currently only ensured below 77 K.[19]

In 2010, the concept of intracavity DFG in vertical-external-cavity surface-emitting lasers (VECSELs) has been demonstrated.[20] Using quasi-phase-matched nonlinear crystals inside their cavity, frequency-converting VECSELs are most favored for the development of compact, room-temperature, stable, and highly efficient THz sources. These lasers have shown great potential to deliver remarkably high THz output power. In this regard, the available high-performance VECSELs,[21,22] also called semiconductor disk lasers (SDLs), can offer outstanding output parameters that are important for efficient intracavity-frequency conversion in a nonlinear crystal. For instance, VECSELs can provide not only remarkably high intracavity powers in the range of a few hundred of watts, but also offer high-power multimode[23] or single-frequency[24] continuous-wave (CW) operation exceeding tens of watts, as well as two-color[25,26] and mode-locked emission.[27]

In recent years, a few VECSEL-based THz sources, referred to as THz-external-cavity surface-emitting lasers (TECSELs), have been demonstrated, commonly utilizing periodically poled lithium niobate (PPLN) crystals[20,26,28–31] and generating non-tunable multimode[31] (with a linewidth of about 30 GHz typical for TECSELs) or, with certain efforts, even single-frequency THz signal.[29] In these laser systems, intracavity etalons are used to enforce a stable two-color operation that is utilized for the generation of CW THz radiation via intracavity-frequency conversion within a nonlinear crystal. To realize THz tunability from such laser sources, specially designed nonlinear crystals with thoughtfully engineered quasi-phase-matching condition should be used. In this respect, the use of aperiodically poled nonlinear crystals can enable phase matching for a wide range of difference frequencies.

In this context, we report the first operation of a practical, room-temperature, widely tunable THz-generating laser based

ADVANCED SCIENCE NEWS
www.advancedsciencenews.com

pssrrl
physica status solidi
www.pss-rapid.com

on an SDL. A significant expansion of the spectral coverage compared to its PPLN-based equivalent is demonstrated, ranging thereby from 0.79 to 1.11 THz based on intracavity DFG in an aperiodically poled lithium niobate (aPPLN) crystal within an SDL.

Figure 1 shows a photograph of the experimental TECSEL setup with the main components labeled. The used metalorganic vapor-phase epitaxy (MOVPE)-grown VECSEL chip consisted of 10 InGaAs quantum wells (QWs), equally spaced by GaAsP barrier layers. The resonant periodic gain structure was arranged by overlapping the QWs with the antinodes of the standing light field. 22.5 AlAs/GaAs layer pairs formed the distributed Bragg reflector (DBR). The laser chip was flip-chip-bonded to a chemical-vapor-deposition-grown diamond heat spreader for optimal temperature management via solid–liquid interdiffusion bonding and then mounted to a water-cooled copper heat sink with temperature set to 18 °C. The chip was pumped by a fiber-coupled diode laser emitting at 808 nm, whereas the VECSEL lased at around 1010 nm.

The VECSEL setup used a V-shaped cavity with a total length of 50 cm, using a highly reflective (HR) concave mirror (M1, radius of curvature 250 mm, 0.05% transmittance) and an HR plane mirror (M2), with an arm length of 20 and 30 cm for the HR mirror and the chip side, respectively. The folding angle on the curved HR mirror amounted to 8°. The diameter of the pump spot was set to be 300 μm, which is 10% smaller than the cavity mode, to ensure the TEM_{00}-mode operation for efficient DFG in an aPPLN crystal. In this cavity, the crystal was placed close to the plane HR mirror (M2), where the Gaussian-beam waist (diameter) of the laser mode reached its minimum of 220 μm. Here, the design was adopted from previous experiments with a PPLN crystal.[20] For broadly tunable THz generation, a 10 mm-long 5 mol% MgO-doped lithium niobate crystal with a slant-stripe aperiodic poling (with a poling period of 50–66 μm and a slanting angle of 67.2°) was used. The crystal was specially designed for efficient THz generation in the range between 0.81 and 1.07 THz.

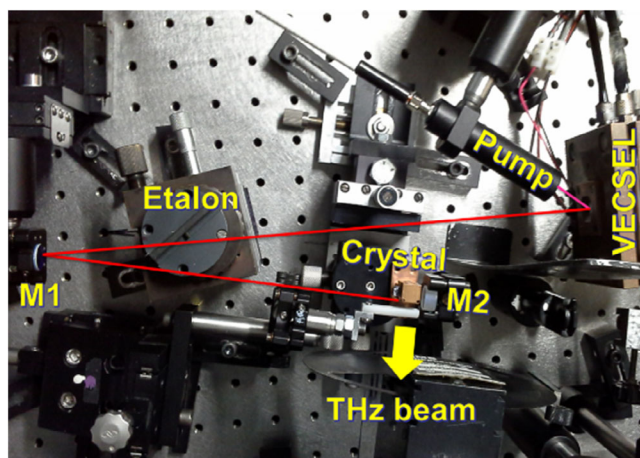A quartz etalon (with a thickness of either 100 or 150 μm) was inserted into the cavity at its Brewster's angle. When an etalon with suitable free spectral range (FSR) at given angle is used, the filtering effect enables two laser mode packages (polarized perpendicularly to both the propagation and the THz emission direction) to oscillate simultaneously in the cavity. As the FSR of the etalons matched the separation needed for ≈0.7 and ≈1 THz output (FSR ≈2.3 and ≈3.5 nm at 1010 nm for 150 and 100 μm etalon, respectively), it was possible to achieve dual-wavelength operation of the VECSEL. A coarse tuning of infrared dual-wavelength emission in the 1007–1012 nm wavelength region (**Figure 2**) with tunable difference frequencies between 0.65 and 1.11 THz was achieved by changing the incidence angle of the etalon used. The spectra were recorded by an ANDO AQ-6315A optical spectrum analyzer with 0.1 nm spectral resolution.

To collect the THz signal obtained via DFG within the aPPLN, a cylindrical polyethylene lens (5 mm focal length) was used to collimate the (vertically) divergent THz beam and then a spherical lens (60 mm focal length) was used to focus it onto a Golay cell's detector aperture. Intracavity powers were deduced through monitoring the total output power behind the concave mirror M1.

For comparison of THz-frequency spectral coverage, the same setup containing a PPLN crystal (with a poling period of 51 μm and a slanting angle of 67.4°) instead of the aPPLN was used. In this case, the PPLN was designed for efficient THz generation at 1.05 THz.

To characterize both TECSELs, input–output measurements (**Figure 3**) and tunability measurements (**Figure 4**) have been carried out. First, a number of performance curves (THz signal vs intracavity power) were recorded, a few of which are exemplarily shown in Figure 3 for a generated frequency of around 1 THz for both configurations (i.e., with the PPLN and aPPLN crystal). The wavelength spacing between the two infrared laser lines was maintained actively for each pump setting to be around the target value (±0.03 nm corresponding to ±0.010 THz in this
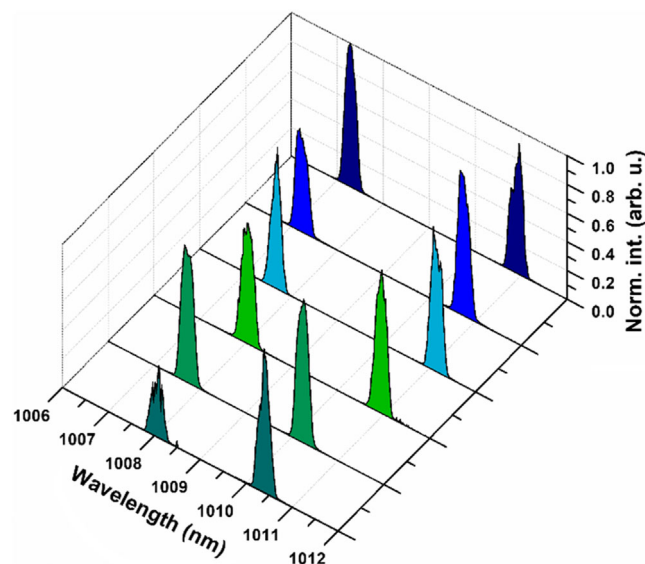

Figure 1. Image of the experimental TECSEL setup with main components labeled. The red and pink lines indicate the 1010 nm intracavity beam and the 808 nm pump beam, respectively. A yellow arrow indicates the generated THz output.

Figure 2. Optical spectra of infrared dual-wavelength emission obtained from the TECSEL utilizing the aPPLN crystal, providing etalon controllable, tunable difference frequency between 0.65 and 1.11 THz (corresponding to a wavelength spacing between 2.22 and 3.76 nm).
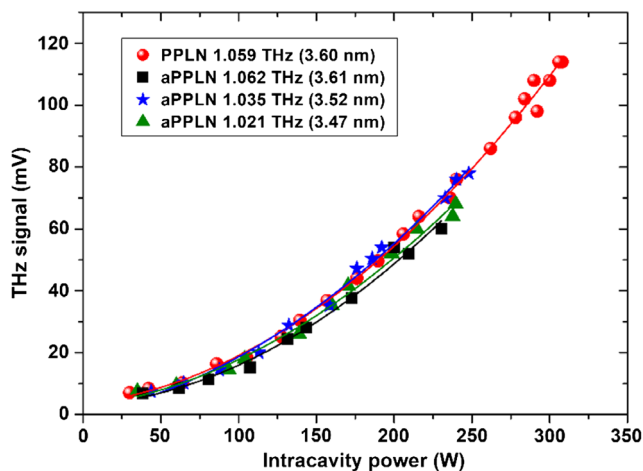
**ADVANCED
SCIENCE NEWS**

www.advancedsciencenews.com

pss rrl
physica status solidi

www.pss-rapid.com

Figure 3. Comparison of the THz output as a function of the intracavity power observed from the TECSELs utilizing the PPLN crystal and the aPPLN crystal at difference frequencies of around 1.05 THz according to the measured wavelength spacings given in the brackets.
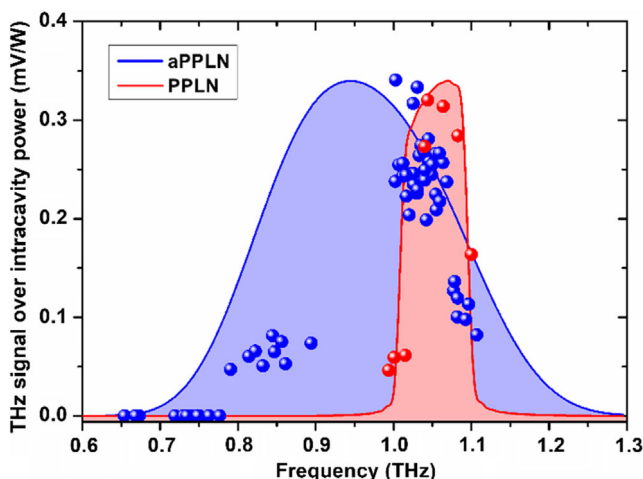

Figure 4. Measured dependence of the THz output (normalized to the TECSEL intracavity power) on frequency for the TECSEL utilizing the PPLN (red) and aPPLN (blue) crystals. For comparison, theoretically expected conversion efficiency curves normalized to the experimental results for the two crystal types are plotted in the background.

wavelength region) by adjusting the etalon throughout these measurements. The measured THz signal output dependencies on intracavity power are easily fitted with quadratic trends expected for the nonlinear-frequency conversion in nonlinear crystals (Figure 3). Our TECSELs demonstrated THz output stability similar to the recently reported TECSEL system in the study by Guoyu et al.[28] For both TECSEL configurations, the further increase in the pump power led to the observation of stronger second-harmonic generation and disappearance of THz generation. This can be attributed to jumps from the TEM_{00} to a multimode operation at higher pump powers. A higher THz output for the PPLN-based TECSEL in comparison with the aPPLN-based one is at the cost of the periodical poling, which allows phase-matching for a specific wavelength only, whereas

aperiodic poling enables phase-matching for a wide range of wavelengths. Thus, the advantage of using either a periodically poled or aperiodically poled crystal within a TECSEL cavity can be exploited with the intended application in mind.

Second, the THz tunability performance of both TECSEL configurations has been investigated. The aPPLN-based TECSEL provided CW tunable-THz output at room temperature in the 0.79–1.11 THz spectral region (Figure 4), whereas the PPLN-based configuration allowed only 0.99–1.10 THz spectral coverage. The tunability measurements were carried out at the same moderate pump power, corresponding to intracavity power levels of ≈150 W. For better clarity and the ease of comparison, the THz output signal was normalized to the corresponding intracavity power in the TECSEL. During the experiment, it was not possible to translate the THz signal to absolute power values due to the lack of a gauged Golay cell. However, based on the estimated intracavity circulating power of about 310 W and, according to the results demonstrated in the study by Scheller et al.,[20] it can be expected that our system can generate THz output in excess of 200 μW. It is worth noting that the full THz tunability range on the high-frequency side has not been fully accessible due to the thickness of the etalon used. Nevertheless, the demonstrated tunability ranges are in good agreement with theoretical predictions. Here, the shapes of the predicted frequency coverage for both crystals are affected by design parameters, such as the size of the laser mode and phase-matching interaction length, that influence the conversion efficiency.

In conclusion, we have experimentally demonstrated for the first time the operation of a room-temperature, CW widely tunable THz-generating laser system. Our device is based on intracavity DFG in a SDL, and the developed laser source allowed us to cover the spectral region between 0.79 and 1.11 THz using a specially designed aPPLN crystal. Furthermore, we have shown that the utilization of the aPPLN crystal within the VECSEL cavity is more favorable in comparison with a PPLN crystal in terms of achievable broad tunability and that it represents an effective approach for the development of tunable THz lasers for a variety of industrial and scientific applications.

Conflict of Interest

The authors declare no conflict of interest.

[1] A. Dobroiu, C. Otani, K. Kawase, *Meas. Sci. Technol.* **2006**, *17*, R161.

[2] P. Jepsen, D. G. Cooke, M. Koch, *Laser Photonics Rev.* **2011**, *5*, 124.

[3] M. Naftaly, N. Vieweg, A. Deninger, *Sensors* **2019**, *19*, 4203.

[4] M. C. Kemp, P. F. Taday, B. E. Cole, J. A. Cluff, A. J. Fitzgerald, W. R. Tribe, *Proc. SPIE* **2003**, *5070*, 44.

[5] J. F. Federici, B. Schulkin, F. Huang, D. Gary, R. Barat, F. Oliveira, D. Zimdars, *Semicond. Sci. Tech.* **2005**, *20*, S266.

[6] C. Weg, W. von Spiegel, R. Henneberger, R. Zimmermann, T. Loeffler, H. G. Roskos, *J. Infrared Millim. Terahertz Waves* **2009**, *30*, 1281.

[7] B. N. Behnken, G. Karunasiri, D. R. Chamberlin, P. R. Robrish, J. Faist, *Opt. Lett.* **2008**, *33*, 440.

[8] M. Humphreys, J. P. Grant, I. Escorcia-Carranza, C. Accarino, M. Kenney, Y. D. Shah, K. G. Rew, D. R. S. Cumming, *Opt. Express* **2018**, *26*, 25805.

[9] S. Verghese, K. A. McIntosh, E. R. Brown, *Appl. Phys. Lett.* **1997**, *71*, 2743.

[10] S. Matsuura, M. Tani, K. Sakai, *Appl. Phys. Lett.* **1997**, *70*, 559.

[11] R. Wilk, F. Breitfeld, M. Mikulics, M. Koch, *Appl. Opt.* **2008**, *47*, 3023.

[12] K. A. Fedorova, A. Gorodetsky, E. U. Rafailov, *IEEE J. Sel. Top. Quantum Electron.* **2017**, *23*, 1.

[13] K. Murate, K. Kawase, *J. Appl. Phys.* **2018**, *124*, 160901.

[14] R. Sowade, I. Breunig, I. C. Mayorga, J. Kiessling, C. Tulea, V. Dierolf, K. Buse, *Opt. Express* **2009**, *17*, 22303.

[15] K. L. Vodopyanov, *Laser Photon. Rev.* **2008**, *2*, 11.

[16] M. S. Vitiello, G. Scalari, B. Williams, P. De Natale, *Opt. Express* **2015**, *23*, 5167.

[17] M. Razeghi, *Int. J. Terahertz Sci. Tech.* **2017**, *10*, 87.

[18] Q. Lu, F. Wang, D. Wu, S. Slivken, M. Razeghi, *Nat. Commun.* **2019**, *10*, 2403.

[19] K. Delfanazari, R. A. Klemm, H. J. Joyce, D. A. Ritchie, K. Kadowaki, *Proc. IEEE* **2020**, *108*, 721.

[20] M. Scheller, J. M. Yarborough, J. V. Moloney, M. Fallahi, M. Koch, S. W. Koch, *Opt. Express* **2010**, *18*, 27112.

[21] A. Rahimi-Iman, *J. Opt.* **2016**, *18*, 093003.

[22] M. Guina, A. Rantamäki, A. Härkönen, *J. Phys. D* **2017**, *50*, 383001.

[23] B. Heinen, T.-L. Wang, M. Sparenberg, A. Weber, B. Kunert, J. Hader, S. W. Koch, J. V. Moloney, M. Koch, W. Stolz, *Electron. Lett.* **2012**, *48*, 516.

[24] F. Zhang, B. Heinen, M. Wichmann, C. Möller, B. Kunert, A. Rahimi-Iman, W. Stolz, M. Koch, *Opt. Express* **2014**, *22*, 12817.

[25] J. Muszalski, A. Broda, A. Trajnerowicz, A. Wójcik-Jedlińska, R. P. Sarzała, M. Wasiak, P. Gutowski, I. Sankowska, J. Kubacka-Traczyk, K. Gołaszewska-Malec, *Opt. Express* **2014**, *22*, 6447.

[26] M. Lukowski, C. Hessenius, M. Fallahi, *IEEE J. Sel. Top. Quantum Electron.* **2015**, *21*, 1700208.

[27] M. A. Gaafar, A. Rahimi-Iman, K. A. Fedorova, W. Stolz, E. U. Rafailov, M. Koch, *Adv. Opt. Photonics* **2016**, *8*, 370.

[28] H. Guoyu, C. Kriso, F. Zhang, M. Wichmann, W. Stolz, K. A. Fedorova, A. Rahimi-Iman, *Opt. Lett.* **2019**, *44*, 4000.

[29] J. R. Paul, M. Scheller, A. Laurain, A. Young, S. W. Koch, J. Moloney, *Opt. Lett.* **2013**, *38*, 3654.

[30] T. A. G. Bondaz, A. Laurain, J. V. Moloney, J. G. McInerney, *IEEE Photon. Tech. Lett.* **2019**, *31*, 1569.

[31] M. Wichmann, M. Stein, A. Rahimi-Iman, S. W. Koch, M. Koch, *J. Infrared Millim. Terahertz Waves* **2014**, *35*, 503.